rhd instruments
flexible cell solutions

Application note

Pouch Cell Cycling with Pressure and Thickness Monitoring in the ComprePouch

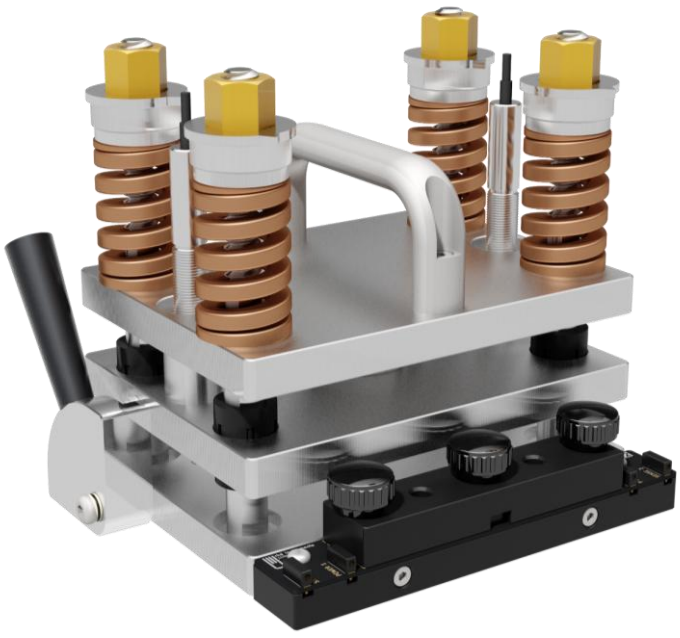

01/2026
Christoffer Folkers-Karlsson
rhd instruments GmbH & Co. KG

Introduction

When cycling pouch cell batteries, the applied pressure has a large impact on their performance and cycle life [1], especially for lithium metal batteries [2] and solid-state batteries [3]. Moreover, local pressure hot-spots can lead to premature ageing and catastrophic failure [4], necessitating not only the measurement of the overall pressure, but of the pressure distribution. On the other hand, *in situ* monitoring of pressure and cell thickness can offer insight into the function of the cell and can be a valuable characterization method [5].

In this application note, a $LiCoO_2$/graphite pouch cell was cycled in the ComprePouch cell fixture [6] using spring packages of different stiffness, while monitoring the pressure, cell thickness, and pressure distribution *in situ*. This was compared to a simulated spring-loaded pressure in the CompreDrive [7].

Experimental

A lithium ion battery pouch cell (ICP606168PRT, Renata AG) with a nominal capacity of 2.7 Ah was used for these tests [5]. It had a $LiCoO_2$ cathode and a graphite anode, with $LiPF_6$ in ethylene carbonate / ethyl methyl carbonate / diethyl carbonate (1 : 1 : 1) electrolyte and a polyethylene / polypropylene separator. The cross-section area of the pouch cell was 36.8 cm^2.

The cell was mounted in a ComprePouch cell fixture fitted with a force sensor and two linear variable differential transformer (LVDT) sensors (rhd instruments GmbH & Co. KG) for pressure and thickness monitoring, respectively [6]. 500 kPa was applied to the cell before placing the ComprePouch in a LabEvent climate chamber (Weiss Technik) at 25 °C. After one hour, the temperature had equilibrated and the pressure was readjusted to 500 kPa. After an additional one-hour rest time, four charge/discharge cycles were performed. This procedure was repeated once for each of the three spring packages of the ComprePouch.

A Biologic SP-240 potentiostat/ galvanostat controlled by EC-Lab 11.63 (Bio-Logic SAS) was used for the charge/discharge cycling. The cell was charged with a C/2 (1.35 A) constant current to 4.2 V, followed by a constant voltage stage to C/10, and then C/2 discharge to 3.0 V.

Additionally, the cell was cycled in the CompreDrive [7] with a simulated spring constant as described previously [8]. The LVDT Distance add-on for the CompreCellPouch was used for the thickness monitoring in this case.

Finally, the cell was also cycled in the ComprePouch with a TekScan 5076 (84 mm × 84 mm, 350 psi) pressure mapping sensor placed under the cell in order to monitor the pressure distribution *in situ*. Polyurethane foam pads (Poron, 1.57 mm, Rogers corporation) were placed below the sensor and above the cell (*cf.* Figure 1 in [9]). These measurements were

performed at room temperature (22 °C) using the "medium" spring package (see **Table 1**). 5x5 interpolation was employed using I-Scan 7.70 (TekScan) to produce the pressure maps shown here.

Edelweiss 1.0 [10] was used for data analysis and for creating the plots in this application note.

Results and Discussion

The results of the charge/discharge cycling of the pouch cell using the "soft", "medium", and "hard" spring packages (**Table 1**) included with the ComprePouch can be seen in **Figure 1**. As no significant differences are visible, the spring stiffness does not seem to have any influence of the electrochemical performance of the pouch cell in the short term.

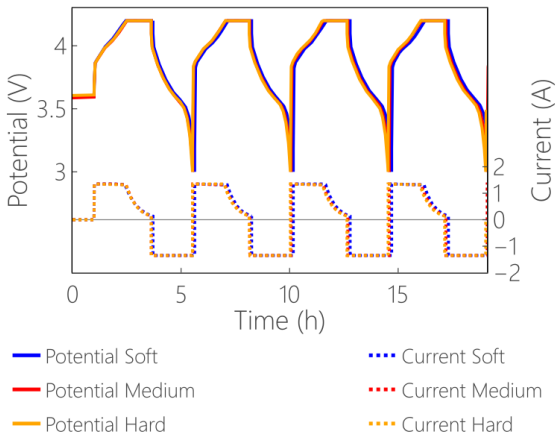

Figure 1. *Potential (solid lines, left y-axis) and current (dashed lines, right y-axis) during charge/discharge cycling with different springs.*

During the charge/discharge cycling, the cell "breathes" as lithium ions are being intercalated in the graphite anode [5, 11]. This cell breathing was monitored *in situ* using LVDT sensors, and was similar for all three spring packages (**Figure 2**), although slightly decreasing with spring stiffness, since the harder springs can withstand the cell breathing to a larger extent.

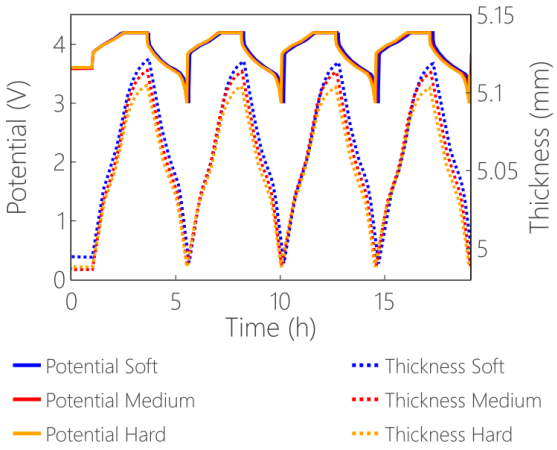

Figure 2. *Potential (solid lines, left y-axis) and thickness variations (dashed lines, right y-axis) during the charge/discharge cycling due to cell breathing.*

Cell breathing forces the springs in the cell fixture to contract, increasing the pressure applied to the pouch cell according to Hooke's law:

$$\Delta F = k \cdot \Delta x$$

where ΔF is the force increase, k is the spring constant, and Δx is the cell breathing. Hence, spring loaded cell fixtures are not "constant pressure" setups, but the pressure experienced by the pouch cell will vary according to the spring constant of the cell fixture as well as the amount of cell breathing. The pressure monitored *in situ* during cycling is shown in **Figure 3**, and varied significantly with the spring stiffness. While the pressure barely changed at all when using the soft springs (1% variation),

Table 1. *Summary of results for each spring package.*

Spring package	Theoretical spring constant (kN/mm)	Experimental spring constant (kN/mm)	Cell breathing (µm)	Pressure variation (kPa)
Soft	0.13	0.15	129	5.5
Medium	1.09	1.01	125	35
Hard	4.60	3.67	116	115

it increased much more when using the medium (7%) and hard springs (23%). Although the cell breathing was almost the same in each case, the same compression resulted in a very different pressure increase depending on the spring stiffness, as expected from the equation above. The amount of cell breathing and pressure variation during cycling is summarized in **Table 1**.

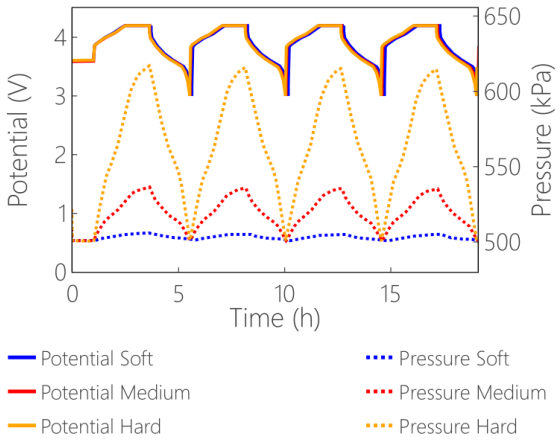

Figure 3. *Potential (solid lines, left y-axis) and pressure variations (dashed lines, right y-axis) during the charge/discharge cycling.*

When the thickness is plotted against the pressure (**Figure 4**), the different slopes according to the respective spring constants are evident. The experimentally evaluated spring constants based on this data are listed in **Table 1** together with the theoretical values (*i.e.* the specified spring constant of each spring multiplied by four, the number of springs in the ComprePouch). For the soft and medium spring packages, the experimental and theoretical values agreed closely, while for the hard spring package, the experimentally determined spring constant was significantly lower. This is caused by a contribution from the ComprePouch cell fixture itself, which can also deform under load. For the softer spring packages, this contribution is insignificant, since the cell fixture is much stiffer in comparison.

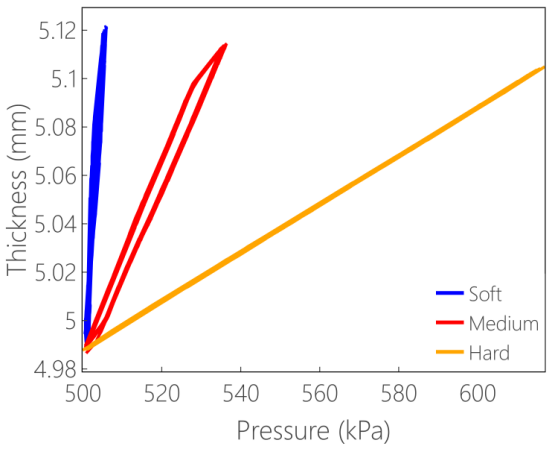

Figure 4. *Cell thickness vs pressure during the charge/discharge cycling.*

As described in a previous application note, the CompreDrive system can simulate a spring-loaded cell fixture [8]. For comparison, the same pouch cell was cycled in the CompreDrive with a simulated spring corresponding to the theoretical medium spring package spring constant (**Table 1**). As shown in **Figure 5**, the cell breathing was almost identical in the simulated (CompreDrive) and real (ComprePouch) case. The potential profile and pressure variation also matched closely.

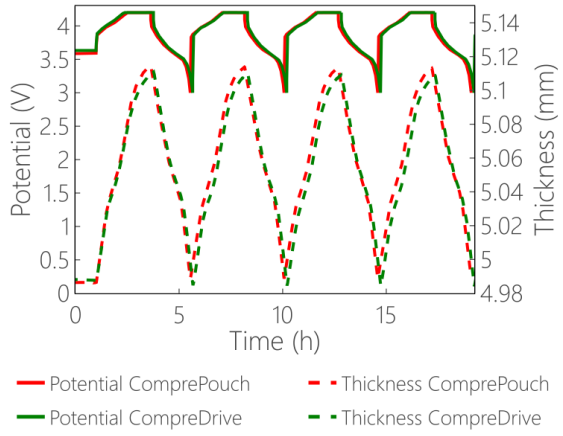

Figure 5. *Potential (solid lines, left y-axis) and thickness variations (dashed lines, right y-axis) during the charge/discharge cycling using the ComprePouch (red) and the CompreDrive with spring simulation (green).*

Finally, using a TekScan pressure mapping sensor, the distribution of the pressure over the pouch cell surface was monitored during cycling in the ComprePouch (**Figure 6**). As noted in a previous application note [9], the highest pressure was observed in the area of the tab welds (towards the top of the images in **Figure 6**, *cf.* Figure 3 in [9]), since that is where the pouch cell is the thickest. For these measurements, foam pads were used to achieve a more even pressure distribution, as discussed in the earlier application note [9]. However, since the foam pads used here were thinner than those employed previously, the pressure was more concentrated to those high spots. The inclusion of the foam pads led to slightly lower increase in pressure and thickness (including the foam pads), since the pads could absorb some of the cell breathing.

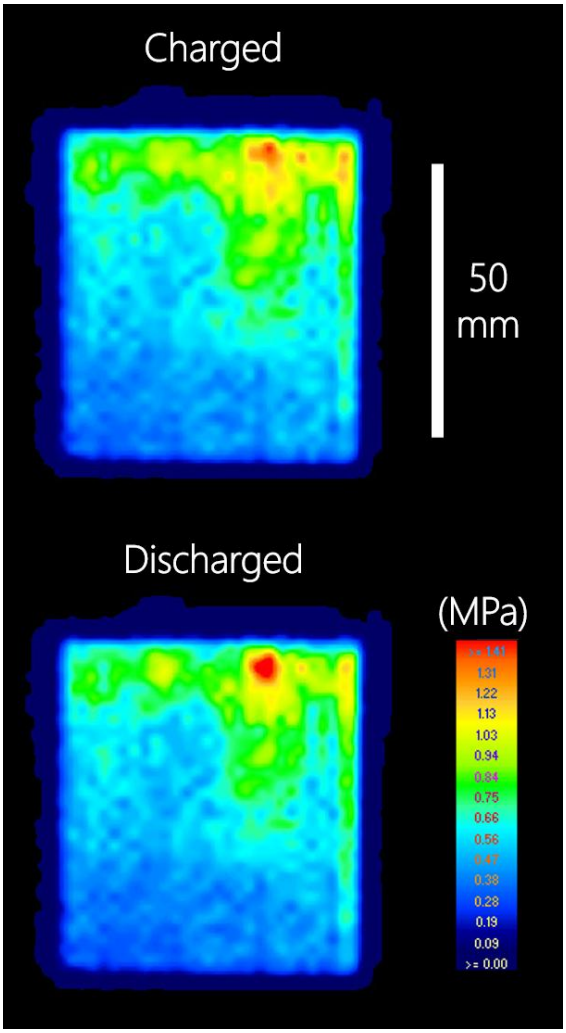

Figure 6. *Pressure distribution over the pouch cell surface after charge (top) and discharge (bottom). The colour indicates the pressure on a scale from 0 (black) to 1.5 MPa (red). The cell is oriented with the tabs towards the top.*

Even though the overall pressure was higher in the charged state, the pressure on the tab welds was larger in the discharged state. This indicates that when the cell is charged, the area under the tab welds expands less than the rest of the cell, which increase in thickness as the cell is charged and can take some of the load, leading to a more even pressure distribution.

Summary

A $LiCoO_2$/graphite pouch cell was cycled under spring-loaded pressure in the ComprePouch using three different spring packages with varying stiffness. The cell breathing during charging caused a pressure increase proportional to the spring constant of the cell fixture. The observed amount of cell breathing was in accordance with a simulated spring-loaded pressure applied in the CompreDrive. Moreover, *in situ* pressure mapping was used during cycling to monitor the evolution of the change in pressure distribution as the cell was charged and discharged.

Literature

[1] M. Wünsch, J. Kaufman and D. U. Sauer, "Investigation of the influence of different bracing of automotive pouch cells on cyclic liefetime and impedance spectra," *Journal of Energy Storage,* vol. 21, pp. 149-155, 2019.

[2] "Application Note: Lithium Metal Solid-State Pouch Cell: Pressure Dependence of Rate Performance," March 2024. https://docs.rhd-instruments.de/ appnotes/application-note_Pouch_Cell_CompreFrame.pdf.

[3] "Application note: All-Solid-State Battery Testing up to 407 MPa using the CompreFrame," October 2025. https://rhd-instruments.de/ magazine/all-solid-state-battery-testing-up-to-407-mpa-using-the-compreframe/.

[4] J. Grabow, J. Klink, R. Benger, I. Hauer and H.-P. Beck, "Particle Contamination in Commercial Lithium-Ion Cells—Risk Assessment with Focus on Internal Short Circuits and Replication by Currently Discussed Trigger Methods," *Batteries,* vol. 9, no. 9, 2023.

[5] C. Karlsson, S. Kranz and B. Huber, "Application Note: In Operando Pouch Cell Thickness Monitoring during Cycling under Controlled Temperature and Pressure," November 2022. https://docs.rhd-instruments.de/ appnotes/application-note_CompreDrive_ Pouch_Cell_Thickness.pdf.

[6] rhd instruments GmbH & Co. KG, "ComprePouch," January 2026. https://rhd-instruments.de/solutions-and-products/for-solid-state-batteries/comprepouch/.

[7] rhd instruments GmbH & Co. KG, "CompreDrive," January 2026. https://rhd-instruments.de/solutions-and-products/for-solid-state-batteries/compredrive/.

[8] C. Karlsson, "Application note: Introducing: True Constant Volume Pouch Cell Cycling," January 2025. https://rhd-instruments.de/magazine/introducing-true-constant-volume-pouch-cell-cycling/.

[9] C. Karlsson, "Application note: Mapping Pouch Cell Pressure Distribution in Operando: CompreCell Pouch × TekScan sensor," June 2024. https://rhd-instruments.de/magazine/mapping-pouch-cell-pressure-distribution-in-operando-comprecell-pouch-x-tekscan-sensor/.

[10] rhd instruments GmbH & Co. KG, "Edelweiss," January 2026. https://rhd-instruments.de/solutions-and-products/for-eis-data-analysis/edelweiss/.

[11] "Application Note: Optical Monitoring of the Lithiation of Graphite in situ," April 2023. https://docs.rhd-instruments.de/appnotes/application-note_Optical_Cell.pdf.